UC San Diego
UC San Diego Previously Published Works

Title

Heterogeneous Formation of Organonitrates (ON) and Nitroxy-Organosulfates (NOS) from Adsorbed α-Pinene-Derived Organosulfates (OS) on Mineral Surfaces

Permalink

https://escholarship.org/uc/item/1tg7t8qq

Journal

ACS Earth and Space Chemistry, 6(12)

ISSN

2472-3452

Authors

Hettiarachchi, Eshani
Grassian, Vicki H

Publication Date

2022-12-15

DOI

10.1021/acsearthspacechem.2c00259

Peer reviewed

Heterogeneous Formation of Organonitrates (ON) and Nitroxy-Organosulfates (NOS) from Adsorbed α-Pinene-Derived Organosulfates (OS) on Mineral Surfaces

Eshani Hettiarachchi and Vicki H. Grassian*

Read Online

ACCESS | Metrics & More | Article Recommendations | SI Supporting Information

ABSTRACT: Organonitrates (ON) and nitroxy-organosulfates (NOS) are important components of secondary organic aerosols (SOAs). Gas-phase reactions of α-pinene ($C_{10}H_{16}$), a primary precursor for several ON compounds, are fairly well understood although formation pathways for NOS largely remain unknown. NOS formation may occur via reactions of ON and organic peroxides with sulfates as well as through radical-initiated photochemical processes. Despite the fact that organosulfates (OS) represent a significant portion of the organic aerosol mass, ON and NOS formation from OS is less understood, especially through nighttime heterogeneous and multiphase chemistry pathways. In the current study, surface reactions of adsorbed α-pinene-derived OS with nitrogen oxides on hematite and kaolinite surfaces, common components of mineral dust, have been investigated. α-Pinene reacts with sulfated mineral surfaces, forming a range of OS compounds on the surface. These OS compounds when adsorbed on mineral surfaces can further react with HNO_3 and NO_2, producing several ON and NOS compounds as well as several oxidation products. Overall, this study reveals the complexity of reactions of prevalent organic compounds leading to the formation of OS, ON, and NOS via heterogeneous and multiphase reaction pathways on mineral surfaces. It is also shown that this chemistry is mineralogy-specific.

KEYWORDS: α-pinene, SOA, nitroxy-organosulfates (NOS), organonitrates (ON), organosulfates (OS), iron oxide, kaolinite
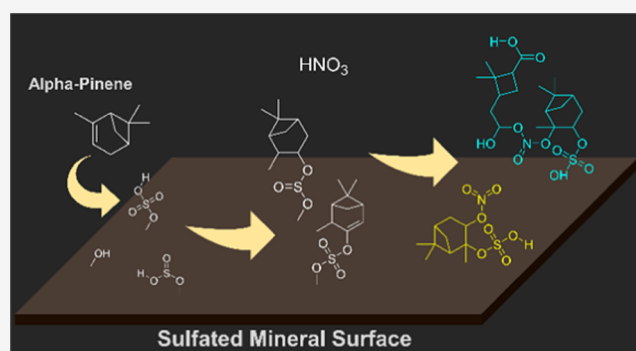
INTRODUCTION

Secondary organic aerosols (SOA) are ubiquitous in the atmosphere and are known to play key roles in climate change, air quality, reduced visibility, and human health.[1−5] Organosulfates (OS, $ROSO_3H$), organonitrates (ON, $RONO_2$), and nitroxy-organosulfates (NOS, $RN_xS_yO_n$) are present within SOA and represent a structurally diverse mixture of compounds found in polluted environments.[6−10] Precursors of these compounds include both biogenic and anthropogenic sources of organic compounds. Primary biogenic precursors are isoprenes, monoterpenes, sesquiterpenes, and aldehydes.[11]

α-Pinene ($C_{10}H_{16}$), a biogenic volatile organic compound, is one of the most abundant atmospheric monoterpenes with an average estimated emission of 66 Tg yr^{-1}.[12−15] Furthermore, α-pinene-derived OS-, ON-, and NOS-SOA along with oxygenated α-pinene derivatives have been detected in ambient air.[16−19] The formation of OS compounds in the atmosphere occurs via several reaction pathways. OS is produced from the photochemical reaction of biogenic hydrocarbons under highly acidic conditions, such as with sulfate aerosols or sulfuric acid, via nucleophilic substitution reactions of sulfate with epoxides in aqueous-phase solutions, with HO radical-involved mechanisms, and via catalytic

reactions with photocatalysts such as TiO_2.[16,17,20−25] Schmidt et al. showed increased formation of OS from methacrolein under illuminated conditions in the presence of road dust.[25] Numerous laboratory studies have been conducted to understand the formation of OS from α-pinene.[22,24,26,27] Surratt et al. reported that the OS is formed when monoterpenes are oxidized in the presence of acidified sulfate aerosol.[22]

Despite the fact that atmospheric OS represents a significant portion of the organic aerosol mass, estimated to be between 3 and 30%,[18,28,29] the formation of ON and NOS from reactions of OS due to nighttime heterogeneous and multiphase chemistry is less understood. Atmospheric ON formation occurs either by OH radical-initiated photochemical reactions or NO_3 radical-initiated nocturnal reactions of anthropogenic

and biogenic volatile organic compounds.[30−35] Reactions of α-pinene with strong atmospheric oxidizers such as O_3 and OH radicals lead to the formation of a range of oxidized α-pinene derivatives that are known as first-generation oxidation products.[4,12,36,37] Some of these compounds are pinonaldehyde, pinonic acid, α-pinene oxide, and structurally diverse organic peroxides. These oxidation products can also act as a reactant in generating atmospheric OS and ON compounds.[38] Oxidation reactions generally occur through photochemical pathways in the presence of sunlight.[30,39] Recently, it was shown that the formation of ON from α-pinene via heterogeneous reactions on mineral surfaces under dry and dark conditions can occur.[40] In the case of NOS formation, its presence in aerosols is almost always observed in the night time. Surratt et al.[22] suggested NOS formation from the reactions of ON with sulfates under acidification, whereas Iinuma et al.[17] suggested the formation of some common NOS such as $C_{10}H_{17}NSO_7$ and $C_{10}H_{18}NSO_7$ occurs during night time. Similar to OS, NOS formation may occur through reactive uptake of epoxides, esterification of hydroxyl and keto groups with sulfuric acid,[41] and/or through radical-initiated processes in wet aerosols.[42] Increased NOS formation due to fireworks has also been previously observed.[11] However, formation pathways for NOS, in general, are less well understood, although their relative abundance and formation pathways involving heterogeneous chemistry in nighttime conditions remain scarce.

In this study, reactions of NO_2 and HNO_3 with α-pinene-OS adsorbed on mineral surfaces hematite (α-Fe$_2$O$_3$) and kaolinite ($SiO_2Al_2O_3(OH)_4$) were studied. The adsorbed α-pinene-OS was produced by exposing α-pinene on mineral surfaces, hematite and kaolinite, first exposed to SO_2. Hematite and kaolinite are major reactive components of mineral dust.[43] Mineral surfaces can interact with gas-phase SO_2,[5,44,455,44,45] leading to the formation of surface products.[46,47] In fact, the interaction of SO_2 on mineral surfaces has been widely studied[48−50] and it has been shown that several surface-adsorbed species form, including sulfate, bisulfate, sulfite, and bisulfite, thereby producing a surface for α-pinene to interact with and facilitating the formation of OS. Additionally, both NO_2 and HNO_3 are found in trace quantities in the atmosphere, primarily via fossil fuel combustion, vehicle exhausts, and agricultural activities.[45−47,51] Due to the higher correlation of atmospheric NO_2 concentrations to traffic, it is used as a traffic-related air pollution marker.[46] Therefore, interactions between α-pinene with mineral dust and trace gas pollutants during dust transport and urban dust episodes can facilitate formation of OS, ON, and NOS.

Given the importance of heterogeneous reactions of atmospheric gases with mineral dust surfaces in the atmosphere and due to the abundance of α-pinene, the role of mineral dust surface chemistry in reactions of α-pinene-OS with atmospheric NO_2 and HNO_3 on hematite and kaolinite surfaces was investigated. This study represents a step forward in understanding the complexity of reactions of volatile and semivolatile organics with trace inorganic gases on mineral surfaces to form multifunctional compounds that can modify the climate impacts of mineral dust.[52] In the current study, experiments were conducted under dark and dry conditions. Although water vapor and adsorbed water play an important role in the chemistry of these surface-mediated reactions,[53] these initial studies were conducted in the absence of coadsorbed water. Both Fourier transform infrared (FTIR)

spectroscopy as an in situ probe of product formation and high-resolution mass spectrometry (HRMS) of solvent-extracted products were used to unravel the complex heterogeneous chemistry occurring on mineral dust surfaces.

■ MATERIALS AND METHODS

Transmission FTIR Experiments and Methods. Transmission FTIR spectroscopy was used to monitor reactions on mineral surfaces at 296 ± 1 K. Additional details of the infrared cell and gas handling system have been previously described.[40,54−58] Mineral particles hematite (α-Fe$_2$O$_3$, 99+%, Fischer Scientific) or kaolinite ($SiO_2Al_2O_3(OH)_4$, Sigma-Aldrich) with a BET surface area of 80 ± 10 and 8.4 ± 0.5 m^2/g, respectively, were heated in an oven at 473 ± 1 K overnight to remove organic contaminants and then pressed onto one half of a tungsten grid (ca. 5 mg). The grid was then placed in the sample IR cell compartment held by two stainless steel jaws. Following the preparation of the mineral sample and placement in the IR cell, the system was evacuated for 4 h using a turbomolecular pump. Mineral surfaces were subsequently exposed to 50% RH water vapor for 2 h to ensure a fully hydroxylated terminated surface. Once hydroxylated, the system was evacuated for another 6 h to remove water vapor in the chamber. After evacuation, the sample was exposed to 100 mTorr of SO_2 (99+%, Sigma-Aldrich) for 20 min under dry conditions (RH < 1%) to obtain an SO_2-exposed mineral surface. The chamber was then evacuated for 4 h to remove gas-phase SO_2 and any weakly bonded SO_2 on the surface. This evacuation ensures that the incoming α-pinene interacts with only strongly adsorbed SO_2 species, and not with any weakly adsorbed SO_2 species. After evacuation, the sample was exposed to 500 mTorr of α-pinene (99+%, Sigma-Aldrich) for 20 min under dry conditions (RH < 1%), and the formation of OS on the surface was studied. The α-pinene sample was degassed at least three times with consecutive freeze−pump−thaw cycles prior to use.

Reactions of gas-phase HNO_3 from the nitric acid vapor taken from a concentrated mixture of H_2SO_4 (~96 wt %)−HNO_3(~70 wt %) 3:1 ratio[59] and NO_2 (26.5 ppm in N$_2$, Airgas) with adsorbed α-pinene-OS on mineral surfaces were studied. First, OS was produced on the surface as described above. The desired pressure of HNO_3 (50 mTorr) or NO_2 (7 mTorr) was then introduced into the IR cell. FTIR spectra were collected over a 4 h period through both halves of the tungsten grid to monitor the gas phase and particle phase. Following adsorption, the system was evacuated overnight. The experiments with HNO_3 were conducted in a different experimental but very similar setup, and instead of stainless steel a Teflon-coated cell was used. Relatively higher concentrations of reactants compared to their atmospheric concentrations were used in this study to determine the feasibility of these types of reactions. Additionally, mass spectroscopic analysis of surface products required these higher concentrations for definitive confirmation as lower concentrations yielded similar HRMS patterns with much lower intensity and higher mass error, suggesting the use of higher concentrations may not impact product formation beyond forming more products.

Prior to and following the exposure to gases, single-beam spectra (250 scans) of the surface and gas phase were acquired using a resolution of 4 cm^{-1} and covering the spectral range of 600−4000 cm^{-1}. This was accomplished by the use of a linear translator with the infrared beam interrogating the portion of

the grid pressed with mineral particles followed by the portion of the grid left blank. Absorption spectra on mineral particles are reported as the difference in the mineral spectra before and after exposure to gases. Absorption bands due to gas-phase components, as measured through the blank half of the tungsten grid under identical conditions, were subtracted to obtain FTIR spectra of adsorbed species only.

HRMS Experiments and Methods. Organic products formed on mineral surfaces following reactions of α-pinene with inorganic gases (SO_2, NO_2, and HNO_3) were analyzed using a direct-injection linear ion trap (ThermoFisher Orbitrap) high-resolution mass spectrometer (HRMS). Adsorbed products were extracted from the hematite or kaolinite solid substrate using methanol (CH_3OH, Fisher Scientific, HPLC grade) as the solvent. Methanol was chosen as the solvent as it produced the best signal for α-pinene standards and OS products relative to other solvents and solvent mixtures (e.g., acetonitrile, ethanol, and their 1:1 mixtures with H_2O). The sample vial, syringe, and all other glassware used in the transfer process were cleaned prior to use with methanol, and Milli-Q water (Millipore Sigma, 18.2 MΩ), and baked in an oven at 773 $\pm$ 1 K to further remove trace organics. Plastic vials used in sample preparation were sonicated in methanol for 60 min and washed thoroughly prior to use. All of the samples were stored at 253 $\pm$ 1 K and analyzed within 48 h of collection. Product stability was tested for up to 10 days in the freeze storage conditions used. It was determined that no transformations of products occurred. Extraction in different solvents confirmed no additional products were formed during the extraction step.

HRMS analysis in both positive electrospray ionization (ESI) ($[M + H]^+$ and $[M + Na]^+$) and negative ESI modes ($[M - H]$) was used. The heated electrospray ionization (HESI) source was operated at 373.15 K. The ESI capillary was set to a voltage of 3.5 kV at 623.15 K. The HESI-Orbitrap MS was calibrated prior to use. Mass spectra were acquired with a mass range of 50–2000 Da. Peaks with a mass tolerance of >5 ppm were rejected. Compositions were calculated with the following element ranges: 12C, 0–60; 1H, 0–150; 16O, 0–25; 14N, 0–5; 32S, 0–5; 23Na, 0–5; 39K, 0–5; 56Fe, 0–5. Tandem mass spectrometry (MS/MS) with a collision energy of 40 eV was used for structure determination.

■ RESULTS AND DISCUSSION

Formation of Organosulfates from α-Pinene on Mineral Surfaces. These experiments were initiated by preparing mineral surfaces with adsorbed OS compounds. This was done by first exposing mineral surfaces to gas-phase SO_2 followed by the exposure of α-pinene as described in the Materials and Methods section. For an SO_2-exposed hematite surface, several species and coordination modes of adsorbed SO_2 species have been observed (Figure S1 and Table S1). In the presence of gas-phase SO_2, these species include molecularly adsorbed SO_2, monodentate and bidentate adsorbed sulfite, adsorbed HSO_3 and $SO_2\cdot H_2O$ complexes, and bidentate and bridging sulfate were observed.[48,60−62] Following evacuation of gas-phase SO_2, previous studies have shown that the adsorption of SO_2 on hematite and other metal oxides forms both adsorbed sulfite and sulfate that remain strongly bound to the surface.[50,62] Similarly, for a sulfated kaolinite surface, adsorbed sulfate species were observed.

Upon exposure to α-pinene, the spectral features for α-pinene on these surfaces become apparent. After evacuation, surface-adsorbed products were retained on the surface (Figure 1). As shown previously, α-pinene weakly adsorbs on hematite
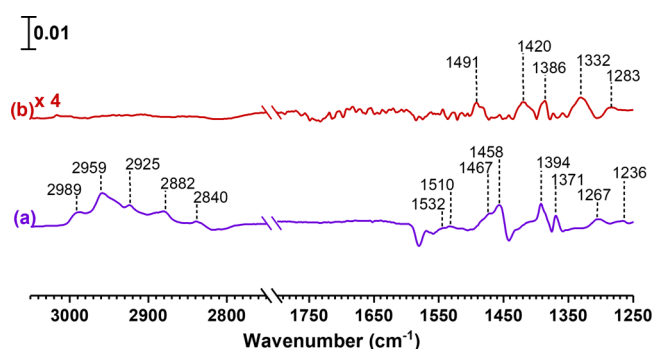

Figure 1. FTIR spectra of surface-bound products from the reaction of α-pinene on (a) sulfated hematite and (b) sulfated kaolinite in the spectral regions from 1250 to 1800 and from 2750 to 3050 cm^{-1}. The absorbance scale is shown in the top left corner.

and undergoes reversible adsorption. Thus, adsorption of α-pinene alone on hematite does not yield any strongly adsorbed product formation. In the case of kaolinite surfaces, it has been shown that α-pinene undergoes oxidation reactions on this surface to yield pinonaldehyde and pinonaldehyde dimer.[40] For hematite, following exposure of SO_2 and α-pinene, there remain adsorbed products following evacuation as evident by the peaks seen in the infrared spectrum. Several features were prominent in the following spectral range: from 2800−3000 cm^{-1} (C−H stretch); 1300−1500 cm^{-1} (C−H bond bending modes); and ~1236 and 1267 cm^{-1} (C−O bond stretch). A concomitant loss of surface hydroxyl groups was observed between 3500 and 3700 cm^{-1} similar to when SO_2 alone was adsorbed. For kaolinite, there were also peaks observed in the spectra albeit of weaker intensity. The most evident ones were from 1250 to 1550 and 3600 to 3900 cm^{-1}. However, given the complexity of products formed on the surface, it is difficult to assign these FTIR spectra to specific molecules. Generally, covalent organosulfates have two strong bands, one at 1415−1370 cm^{-1} and the other at 1200−1185 cm^{-1}, both of which are due to the stretching vibrations of the SO_2 group.[63] The peaks arising due to adsorbed sulfate and sulfite overlap in the same region as OS bond vibrations.[64]

To obtain additional molecular-level insights into these surface-bound products, compounds were solvent-extracted from the surface and further analyzed for product identification using HRMS (Figure 2). The HRMS patterns of surface products collected in neg-ESI mode from the reactions of α-pinene with adsorbed SO_2 species on hematite indicated the presence of several OS compounds (Figure 2 and Table 1).

These identified OS compounds correspond to $C_{10}H_{17}SO_3$ (compound **1**, m/z = 217.09), $C_{10}H_{17}SO_4$ (compounds **2** and **3**, m/z = 233.09), $C_{10}H_{15}SO_3$ (compound **4**, m/z = 215.07), $C_{10}H_{17}SO_5$ (compound **5**, m/z = 249.08), and $C_{10}H_{15}SO_4$ (compound **6**, m/z = 231.07). The structures of these compounds were confirmed via tandem mass spectrometry. Furthermore, neither oxygenated α-pinene derivatives nor unreacted α-pinene were observed via HRMS analysis. For kaolinite, several OS compounds were identified from both neg- and pos-ESI modes. In neg-ESI mode, apart from compounds **1**−**6**, two new OS were identified. These are $C_{20}H_{31}SO_7$ (compound 7, m/z = 415.18) and $C_{30}H_{47}SO_7$ (compound 8, m/z = 551.31). In pos-ESI mode, $C_{10}H_{17}SO_5$
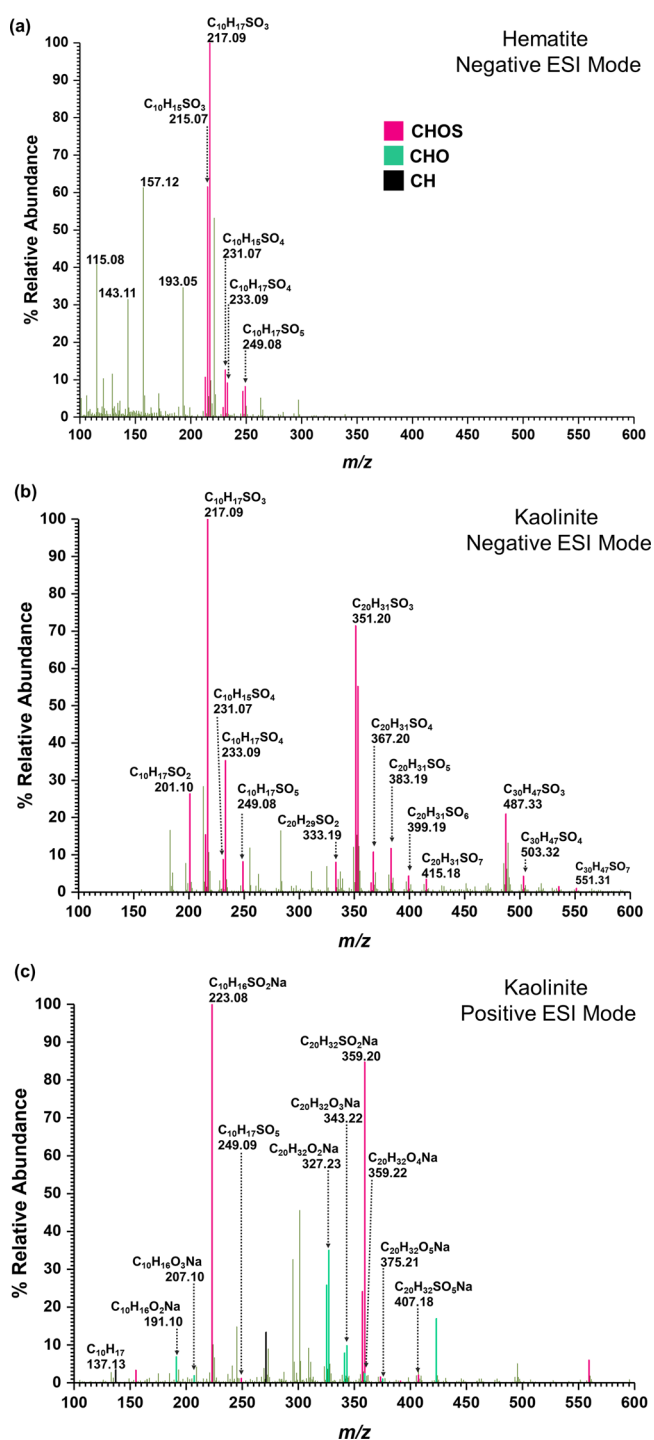
Figure 2. HRMS patterns in both positive $[M + H]^+$ and negative $[M - H]^-$ ESI modes, of surface-bound products from the reaction of α-pinene with sulfated mineral surfaces on (a) hematite and (b, c) kaolinite. HRMS pattern for hematite in positive-ESI mode did not produce any analyte peaks. Confirmed peaks are color-coded according to heteroatoms. Pink box solid—CHOS; green box solid—CHO; black box solid—CH.

The presence of both compounds **2** and **3** was confirmed via MS/MS analysis. Similarly, the structure for **9** was determined based on its major fragments at $m/z = 223.08$ ($C_{10}H_{16}SO_2Na$) and 191.10 ($C_{10}H_{16}O_2Na$), which suggested the presence of a pinonaldehyde moiety. Table S2 provides detailed information on the mass fragmentation of identified compounds. Similar OS compounds were identified in various field and chamber studies, suggesting the formation of these OS compounds from α-pinene occurs in a broader environment.[19,26,27,41,65−67]
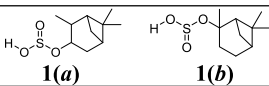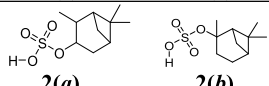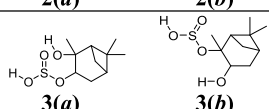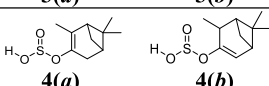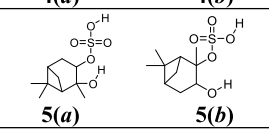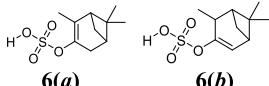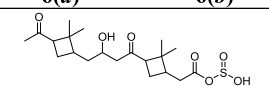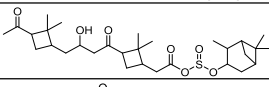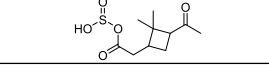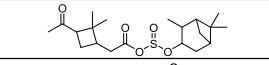
Formation pathways of these OS compounds are facilitated on these mineral surface mechanisms (Scheme 1).[70,73−77] Briefly, the adsorbed SO_2 species on mineral surfaces can interact with π bonds of α-pinene in the gas phase, producing a series of OS compounds.[26,27,78,79] Compounds **1** and **2** can form via carbocation formation from the reaction of α-pinene with adsorbed sulfate/sulfite on mineral surfaces. The reaction of α-pinene π bonds with acid groups such as sulfate was previously proposed.[17] The carbocation can react with adsorbed sulfite or sulfate species on mineral surfaces to form the isomers of compounds **1** or **2**, respectively (Scheme 1a). Compounds **3** and **5** can form via the interaction of π bonds in α-pinene with the surface redox sites/surface hydroxyl groups on mineral surfaces, leading to the formation of pi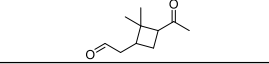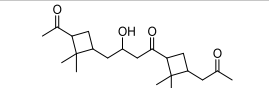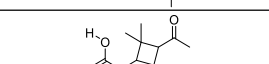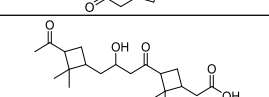nene oxide-like species. A similar reaction is prominent in limonene (an isomer of α-pinene) forming limonene oxide;[80] here, the interactions are expected to be weaker for α-pinene given no α-pinene oxide was observed from its interactions with mineral surfaces.

The reaction of adsorbed sulfite or sulfate species on mineral surfaces with one of the two epoxide carbons on α-pinene can yield compound **3** or **5**. The presence of peaks corresponding to HSO_3^- ($m/z = 80.97$), SO_3 ($m/z = 79.95$), and HSO_4^- ($m/z = 96.96$) in the HRMS fragmentation pattern of $m/z = 233.09$ further confirms the formation of both sulfate and sulfite groups containing α-pinene-derived OS compounds.

Two formation pathways are proposed for compound **4**. First, the dehydration of compound **3** yields compound **4**. Second, the loss of 2H atoms from compound **1** in the mass spectrometer can yield $m/z = 215.07$. Similarly, compound **6** can form from the dehydration of compound **5** or the removal of 2H atoms from compound **2** during the HRMS analysis (Scheme 1b). Dehydration of compounds **3** and **5** from compounds **4** and **6**, respectively, can occur either on mineral surfaces or during the HRMS analysis. Duporté et al. observed an OS at 249 (compound **5** in this study) dehydrating to an OS at 231 (compound **6**) during MS analysis.[27]

On kaolinite, α-pinene derivatives pinonaldehyde (**11**) and pinonaldehyde dimer (**12**) are formed[40] and further oxidized to form their respective acids (compounds **13** and **14**). Formation of pinonaldehyde and pinonaldehyde dimer upon exposure to kaolinite surfaces is explained in detail in our previous study.[40] Briefly, these are from the dihydroxylation of double bond on α-pinene followed by glycol cleavage on the kaolinite surface. Compound **7** can be expected to form from the reaction of adsorbed sulfites with compounds **11** and **12**, respectively. In this case, adsorbed sulfites act as a nucleophile and attack aldehyde carbon on either compound **9** or **7**. Compound **9** can also form from the olefinic cleavage of compound **4** in a similar way to pinonaldehyde formation from α-pinene. Compound **8** can be expected to form due to the reaction between compounds **14** and **1**. Similarly, compound **10** may be formed due to the reaction between compounds **13** and **1** (Scheme 1c,d). Therefore, these results show the

(compound **9**, $m/z = 249.09$) and $C_{20}H_{32}SO_5Na$ (compound **10**, $m/z = 407.18$) along with pinonaldehyde ($C_{10}H_{16}O_2Na$, compound **11**, $m/z = 191.10$), pinonalehyde dimer ($C_{20}H_{32}O_4Na$, compound **12**, $m/z = 359.22$), pinonic acid ($C_{10}H_{16}O_3Na$, compound **13**, $m/z = 207.10$), and $C_{20}H_{32}O_5Na$ (compound **14**, $m/z = 375.21$) were observed.

Table 1. Identified Surface Products Using HRMS and MS/MS in Either Positive $[M + H]^+$ or Negative ESI $[M − H]^−$ Modes from the Reactions of α-Pinene on Sulfated Mineral Surfaces[abcd]

| ID	Observed Formula, ESI Mode (Molecular Formula)	m/z	Proposed Structure	Hematite	Kaolinite	Previously reported in field/ laboratory studies [a]
1	$C_{10}H_{17}SO_3$, − $(C_{10}H_{18}SO_3)$	217.09	1(a) 1(b)	√[b]	√	N/A[c]
2	$C_{10}H_{17}SO_4$, − $(C_{10}H_{18}SO_4)$	233.09	2(a) 2(b)	√	√	N/A
3	$C_{10}H_{17}SO_4$, − $(C_{10}H_{18}SO_4)$	233.09	3(a) 3(b)	√	√	N/A
4	$C_{10}H_{15}SO_3$, − $(C_{10}H_{16}SO_3)$	215.07	4(a) 4(b)	√	√	N/A
5	$C_{10}H_{17}SO_5$, − $(C_{10}H_{18}SO_5)$	249.08	5(a) 5(b)	√	√	22,26,27,42,65,67–69
6	$C_{10}H_{15}SO_4$, − $(C_{10}H_{16}SO_4)$	231.07	6(a) 6(b)	√	√	26,27
7	$C_{20}H_{31}SO_7$, − $(C_{20}H_{32}SO_7)$	415.18		−−[d]	√	N/A
8	$C_{30}H_{47}SO_7$, − $(C_{30}H_{48}SO_7)$	551.31		−−	√	N/A
9	$C_{10}H_{17}SO_5$, + $(C_{10}H_{16}SO_5)$	249.09		−−	√	22,24,41,65–67,69
10	$C_{20}H_{32}SO_5Na$, + $(C_{20}H_{32}SO_5)$	407.18		−−	√	N/A
11	$C_{10}H_{16}O_2Na$, + $(C_{10}H_{16}O_2)$	191.10		−−	√	40,68,70–72
12	$C_{20}H_{32}O_4Na$, + $(C_{20}H_{32}O_4)$	359.22		−−	√	40,73–75
13	$C_{10}H_{16}O_3Na$, + $(C_{10}H_{16}O_3)$	207.10		−−	√	22,42,68,71,72,75,76
14	$C_{20}H_{32}O_5Na$, + $(C_{20}H_{32}O_5)$	375.21		−−	√	74–77

[a]One or more of the compound, molecular formula, and m/z has been reported. [b]√ = Detected in HRMS. [c]N/A = Not available. [d]−− = Not detected in HRMS.

formation of these multiple OS surface products from reactions of α-pinene with adsorbed SO_2 species on mineral surfaces in dark and dry conditions, in the absence of strong atmospheric oxidizers such as HO radicals and O_3, thus underscoring the unique role the surface plays. These compounds interact with adsorbed SO_2 species on surfaces, yielding a more complex mixture of SOAs. One such possible interaction is the relatively well studied sulfate ester and OS formation from pinonaldehyde.[16,22,26,27,41,66]

Reactions of Gas-Phase Nitric Acid and Nitrogen Dioxide with Adsorbed α-Pinene-OS. In these FTIR experiments, the mineral surfaces were prepared as described above to form adsorbed OS. These surfaces were then exposed to either gas-phase HNO_3 or NO_2 for several hours (4 h). The evacuated surfaces are shown in Figure 3. Upon exposure to HNO_3, new spectral features around 1500−1550 and ~1300 cm$^{−1}$ started to appear on the hematite surfaces. These are attributed to different types of adsorbed nitrate species.[58] Moreover, asymmetric and symmetric stretching vibrations of the NO_2 group of ON occur at 1615−1660 and 1270−1285 cm$^{−1}$.[63] In addition to these, peaks at 2878, 2961, and 2986 cm$^{−1}$ were attributed to C−H stretching modes, and peaks at 1472 and 1458 cm$^{−1}$ were assigned to C−H bending modes. In contrast, for kaolinite surfaces, only weaker spectral features corresponding to organics at 2875, 2927, and ~1325 cm$^{−1}$ were observed. However, a strong band at 3233 cm$^{−1}$ was

Scheme 1. Proposed Formation Pathways for Several of the Compounds Observed in HRMS Compounds (a) 1 and 2, (b) 3, 4, 5, and 6 on Mineral Surfaces and (c) 9, 10, 11, and 13, (d) 7, 8, 12, and 14 on Kaolinite Surfaces
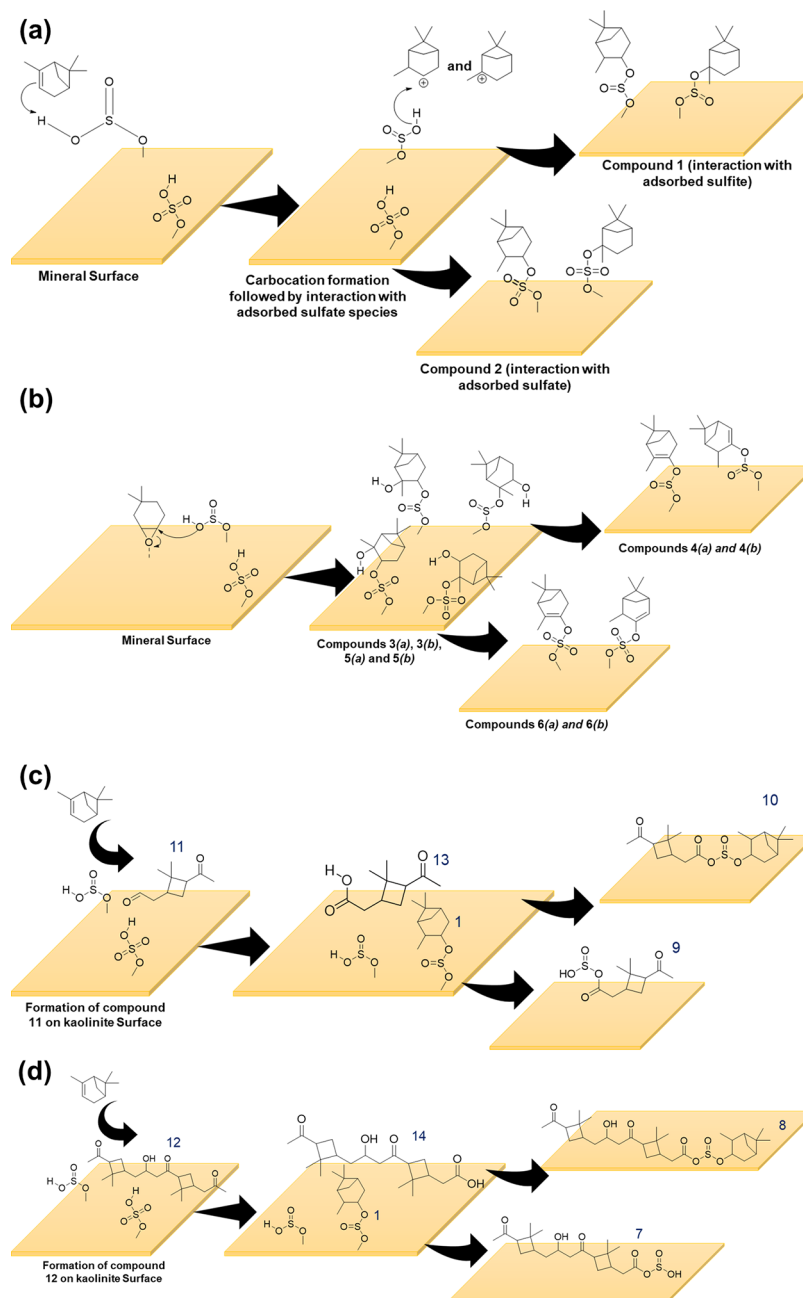
observed, suggesting the presence of hydrogen-bonded networks that could include the presence of alcohols, and/or protonated carboxylic acids. Upon exposure to NO_2, minimal changes of spectral features from OS adsorbed on hematite were observed at ~1370−1420 cm^{-1}, but a weak band at 1550 cm^{-1} was seen.

For kaolinite, spectral features around 1300−1450 cm^{-1} as well as weaker features at ~2967 cm^{-1} were observed, suggesting the presence of C−H bonds on the surface. Furthermore, a strong band at 3488 cm^{-1} was observed, indicating the presence of O−H groups. However, given the complexity of products formed on the surface for specific compounds, these surface-bound products were extracted and analyzed using HRMS and MS/MS to identify products and for structural determination.

Product Formation from the Reactions of Adsorbed α-Pinene-OS with Gas-Phase HNO_3. The HRMS patterns collected in both neg- and pos-ESI modes of surface products from reactions of HNO_3 with adsorbed OS species on hematite indicated the presence of several OS compounds, ON compounds, and NOS compounds (Figure 4a,b, Table 2). Apart from the presence of compounds 1 and 2, a new OS, Compound 15 ($C_9H_{14}SO_6$, sulfated pinalic-3-acid, m/z = 369.12 for $C_{12}H_{26}SO_9Na$) was observed. Compound 15 was observed as a sodated cluster of three methanol units and with a major fragment at 365.09 for $C_{12}H_{22}SO_9Na$. Furthermore, m/z = 233.09 was assigned only to compound 2, as no indication of SO_3 was shown on its MS/MS fragmentation. Two major ON products were identified. Compound 16 ($C_{10}H_{16}NO_3$, m/z = 198.15) was identified with its major
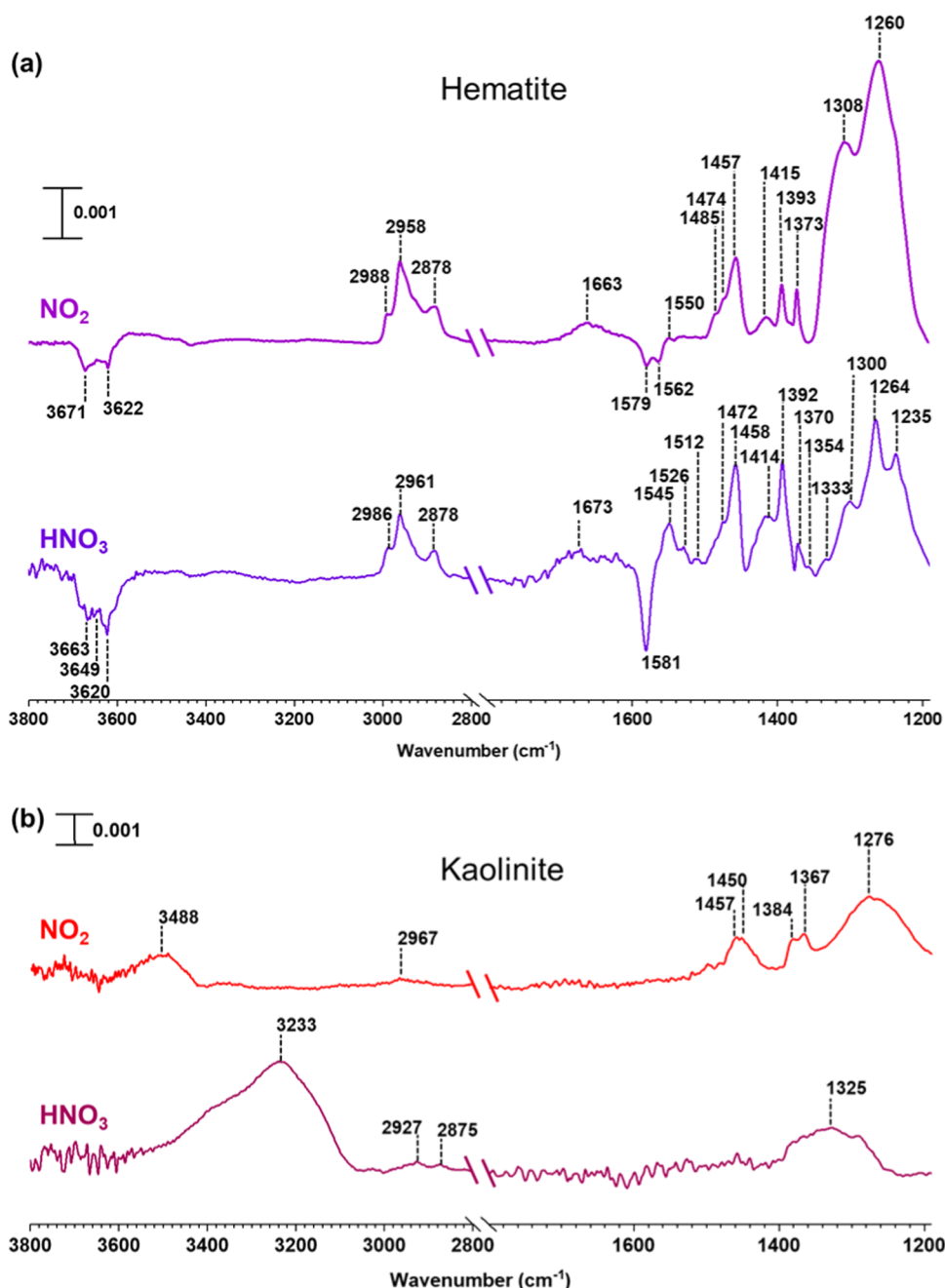
Figure 3. FTIR spectra of surface-bound products from the reaction of adsorbed α-pinene-OS with either HNO_3(vapor) or NO_2(g) on (a) hematite and (b) kaolinite in the spectral regions from 2800 to 3800 cm^{-1} and from 1190 to 1800 cm^{-1}. The absorbance scale is shown in the upper left for each surface.

fragment 166.12 for $C_{10}H_{16}ON$. Compound **17** ($C_{20}H_{34}NO_3$, $m/z = 336.25$) was identified with major fragments at 320.26 for $C_{20}H_{34}NO_2$, 302.25 for $C_{20}H_{32}ON$, and 168.14 for $C_{10}H_{18}ON$. Two NOS were identified. Compound **18** ($C_{10}H_{16}NSO_7$, $m/z = 294.06$) was identified with a major fragment at 278.07 for $C_{10}H_{16}NSO_6$. Compound **19** ($C_{19}H_{32}NSO_{10}$, $m/z = 595.29$ for $C_{23}H_{49}NSO_{14}$) was identified as a 4 methanol-units cluster. Its major fragments were at $m/z = 579.29$ for $C_{23}H_{49}NSO_{13}$ and 302.14 for $C_{14}H_{24}NSO_4$. A smaller m/z at 467.18 for $C_{19}H_{33}NSO_{10}$ (compound **19** without methanol units clustered) was also observed. The nonsulfated molecule of compound **15**, pinalic-3-acid,[3,68,81−85] has been widely observed in the environment as well as in laboratory experiments. Similarly, compounds with

similar molar weight/formula to compounds **16, 17, 18,** and **19** have been previously observed in both laboratory experiments and the field.[11,19,22,40,42,68,69,71,72,86−89]

Despite wide observations of pinalic-3-acid in the environment, the mechanistic details of how this compound forms, as well as that of compound **15**, are unclear. Pinalic-3-acid forms via the ozonolysis of α-pinene. In the current study, it can be speculated that HNO_3/adsorbed nitrates on hematite may induce the formation from the OS present on the hematite surface. Given that HSO_4^- is a good leaving group,[90] the formation of sulfated pinalic-3-acid (**15**) can occur either via oxidation of sulfated α-pinene, or sulfation of formed pinalic-3-acid by the surface-adsorbed sulfate species. Further research studies are recommended to better understand the underlying
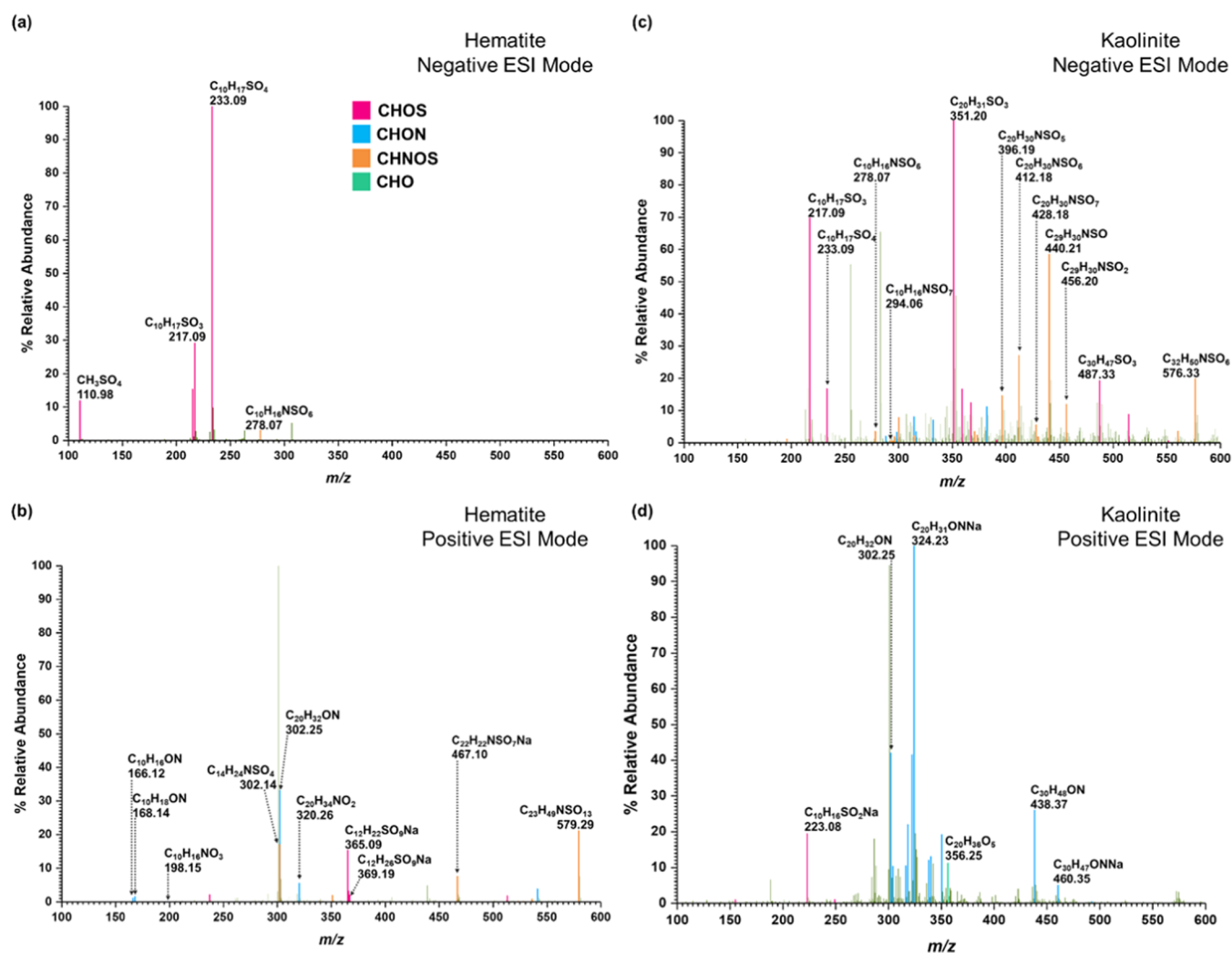
Figure 4. HRMS patterns in both positive $[M + H]^+$ and negative $[M - H]^-$ ESI modes of surface-bound products from the reactions of adsorbed α-pinene-OS with HNO_3(vapor) on (a, b) hematite and (c, d) kaolinite. Confirmed peaks are color-coded according to heteroatoms. Pink box solid—CHOS; blue box solid—CHON; orange box solid—CHNOS; green box solid—CHO; black box solid—CH.

mechanisms of formation of compound **15** on mineral surfaces in the presence of HNO_3.

A smaller quantity of compound **16** was observed in the study. Compound **16** was previously observed in our studies forming from reactions of α-pinene with adsorbed nitrates on hematite surfaces.[40] However, here, nitrate is likely to act as a nucleophile on either compound **1** or **2** followed by the leaving of sulfate/sulfite group as their respective acid, resulting in a C=C on compound **16** (Scheme 2). Sulfate species are known to be good leaving groups.[90]
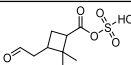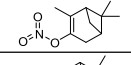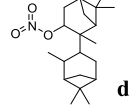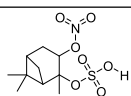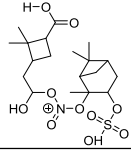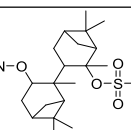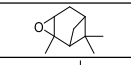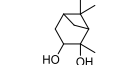
Formation of compound **17** suggests that α-pinene-OS may undergo dimerization as well. Both α- and β-pinene dimerization has previously been studied.[91,92] We speculate this is due to the interaction of surface hydroxyl groups with pi hydrogens in the α-pinene moiety of compounds **4**, **6**, and **16**, a carbocation forms and undergoes dimerization with compound **4** or **6** on the surface followed by elimination of H_2SO_3/H_2SO_4. However, the exact formation pathway remains unclear. Moreover, it is worth investigating whether their formation is possible at low α-pinene concentrations.

The formation of compound **18** is proposed to occur via the addition of an HNO_3 molecule on the double bond of either compound **4** or **6**. It is expected that the sulfite group in

compound **4** is oxidized by HNO_3 molecules in the system. Compound **19** likely forms via reactions between compound **15** (or pinalic-3-acid) and compound **18**. The nitrate group in compound **18** may react with either $-COOSO_3$ ($-COOH$ in pinalic-3-acid) or aldehyde end. However, we propose the reaction undergoes via aldehyde end due to the formation of fragment 302.14 for $C_{14}H_{24}NSO_4$. This fragment may be possible if the reaction occurs via the aldehyde end. A smaller peak at $m/z = 547.14$ for $C_{19}H_{33}NS_2O_{13}$ was also observed, suggesting the presence of two 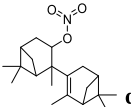sulfate groups in the same molecule. However, it was not listed as a separate compound due to the lower occurrence. Despite the fact that our experimental evidence suggests the possible formation pathway for Compound **19** is as shown in Scheme 2c, given the nitrate esters are usually considered to be weak nucleophiles, a more detailed investigation of high molecular weight NOS formation, such as Compound **19**, is warranted.

Five α-pinene-OS products were observed on kaolinite surfaces after exposure to HNO_3 along with three ON and two NOSs. The OS are compounds **1**, **2**, **3**, **8**, and **9**. The ON, compound **20** ($C_{20}H_{32}NO_3$, $m/z = 334.24$, pos and $C_{20}H_{30}NO_3$, $m/z = 332.22$, neg), was identified. Another possible ON, compound **21** ($C_{30}H_{47}NO_3Na$, $m/z = 492.34$),

Table 2. Identified Surface Products Using HRMS and MS/MS in Either Positive $[M + H]+$ or Negative ESI $[M − H]^-$ Modes, from the Reactions of Adsorbed α-Pinene-OS with Either HNO_3 or NO_2 on Mineral Surfaces[abcde]

| ID	Observed Formula, ESI Mode (Molecular Formula)	m/z	Proposed Structure	Hematite		Kaolinite	Previously reported in field/ laboratory studies [a]
				AP+HNO_3	AP+NO_2	AP+HNO_3	
15	$C_{12}H_{26}SO_9Na$, + ($C_9H_{14}SO_6$)	369.19		√ [b]	-- [c]	--	3,24,85,86,65,68,69,72,81–84
16	$C_{10}H_{16}NO_3$, + ($C_{10}H_{15}NO_3$)	198.15		√	√	√	40,71,72
17	$C_{20}H_{34}NO_3$, + ($C_{20}H_{33}NO_3$)	336.25	d	√	--	--	86
18	$C_{10}H_{16}NSO_7$, - ($C_{10}H_{17}NSO_7$)	294.06		√	--	√	11,19,22,42,68,69,87–89
19	$C_{23}H_{49}NSO_{14}$, + ($C_{19}H_{32}NSO_{10}$)	595.29 and 467.18		√	--	--	22
20	$C_{20}H_{32}NO_3$, + $C_{20}H_{30}NO_3$, - ($C_{20}H_{31}NO_3$)	334.24, + 332.22, -	d	--	√	√	86
21	$C_{30}H_{47}NO_3Na$, + ($C_{30}H_{47}NO_3$)	492.34	N/A	--	--	√	N/A [e]
22	$C_{20}H_{32}NSO_7$, - ($C_{20}H_{33}NSO_7$)	430.19		--	--	√	N/A
23	$C_{32}H_{50}NSO_6$, - ($C_{32}H_{51}NSO_6$)	576.33	N/A	--	--	√	N/A
24	$C_{10}H_{17}O$, + ($C_{10}H_{16}O$)	153.13		--	√	--	26,40,71,72
25	$C_{10}H_{18}O_2Na$, + ($C_{10}H_{18}O_2$)	193.12		--	√	--	72

[a]One or more of the compound, molecular formula, and m/z has been reported. [b]√ = Detected in HRMS. [c]-- = Not detected in HRMS. [d]Best matched structure with HRMS, MS/MS data, and molecular formula. [e]N/A = Not available.

with three α-pinene moieties was identified in positive-ESI mode. Compound **21** produced several key fragments. Among these are 460.35 for $C_{30}H_{47}ONNa$, 438.37 for $C_{30}H_{48}ON$, and 324.23 for $C_{20}H_{31}ONNa$. Compound **18** ($C_{10}H_{16}NSO_7$, m/z = 294.06) was identified in the neg-ESI mode with a major fragment at 278.07 for $C_{10}H_{16}NSO_6$. Another NOS, compound **22** ($C_{20}H_{32}NSO_7$, m/z = 430.19), in the neg-ESI mode produced a series of fragments at 428.18 ($C_{20}H_{30}NSO_7$), 412.18 ($C_{20}H_{30}NSO_6$), and 396.19 ($C_{20}H_{30}NSO_5$). A major peak was observed at 576.33 with the formula of $C_{32}H_{50}NSO_6$, and its fragments at 456.20 for $C_{29}H_{30}NSO_2$, 440.21 for $C_{29}H_{30}NSO$, and 351.20 for $C_{20}H_{31}SO_3$ were assigned to belong to the same compound (**23**). The formula or the structure of compound **23** was not identified in these studies. Many studies have reported the formation of high molecular weight ON, OS, and NOS in the environment.[11,19,22,68,69,86−88] Similar to these studies, most interesting is that in this current study, the formation of a unique mixture of SOAs on these surfaces underscores the complexity of these reactions.

Furthermore, highlighting the importance of mineral surfaces, formation of a C_9 compound (**15**) facilitating further SOA formation of a C_{19} compound (**19**) is observed only with hematite surfaces in the presence of HNO_3. Hematite and kaolinite surfaces represent both redox-active minerals and common clay minerals, respectively. The differences in the surface chemistry reflect the different surface properties— surface structure, surface hydroxyl group density, redox active sites, and specific surface planes. The details of these different properties and how they play a role in the reaction mechanism have yet to be fully discerned (Figure 5).

Product Formation from the Reactions of Adsorbed α-Pinene-OS with Gas-Phase NO_2. Reactions of NO_2 with adsorbed α-pinene-OS on hematite surfaces produced a series of compounds. Some of these compounds were also observed during reactions of α-pinene-OS with HNO_3 and others are unique. Some of these differences may arise from the lower acidity resulting in the mineral surface upon exposure to NO_2 than when exposed to HNO_3 as acid-catalyzed reactions can

Scheme 2. Proposed Formation Pathways for Compounds Identified in HRMS: (a) Compound 15, (b) Compound 16, (c) Compound 18, and (d) Compound 19 on Mineral Surfaces
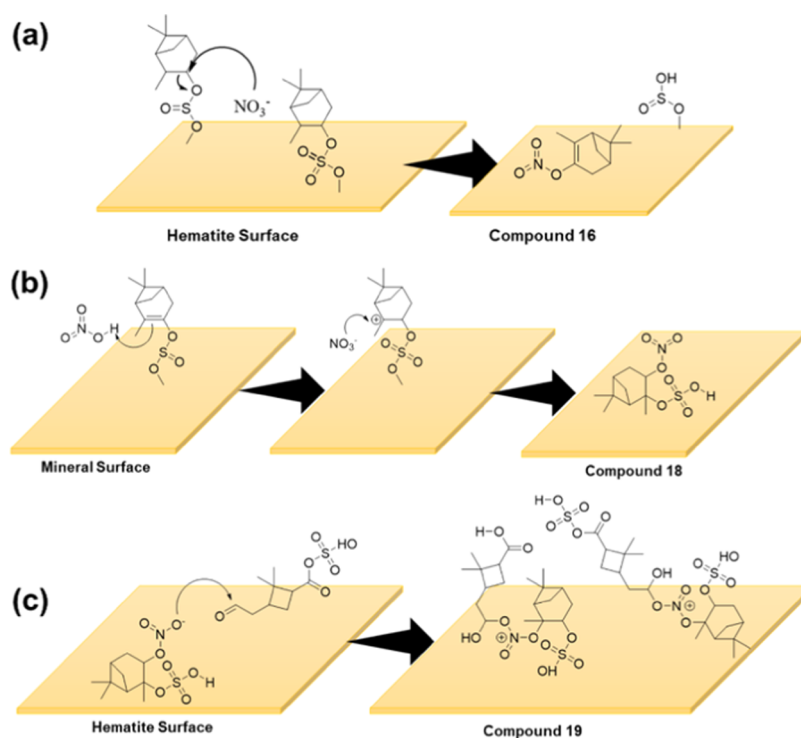
induce formation of products in the presence of HNO_3 vapor. Among these were two OS, compounds **2** and **3**, two ON, compounds **16** and **20**, and four oxidized α-pinene derivatives, compounds **11**, **13**, **24** ($C_{10}H_{17}O$, m/z = 153.13 and $C_{10}H_{16}ONa$, m/z = 175.11, α-pinene oxide), and **25** ($C_{10}H_{18}O_2Na$, m/z = 193.12, α-pinene diol). Compounds **2** and **3** were identified in both negative and positive ESIs modes. Furthermore, a range of peaks containing NSO groups were identified in positive-ESI mode, suggesting the formation of NOS during these reactions. These peaks were 535.31 for $C_{19}H_{30}NSO_{13}Na$, 362.07 for $C_{17}H_{16}NSO_6$, 321.04 for $C_{16}H_{12}NSO_3Na$, 279.06 for $C_6H_{17}NSO_9$, and 113.96 for $CHNSO_2Na$. Although none of these peaks were assigned to a particular compound, it is important to note that both C_{17} and C_{16} compounds have been previously observed from α-pinene SOAs.[85,86,93] Similarly, reactions of adsorbed α-pinene-OS on kaolinite surfaces with NO_2 produced a mixture of different SOAs. The OS **1**, **2**, **3**, **7**, **9**, and **10** were observed. The oxygenated α-pinene derivatives, compounds **11**, **12**, and **13**, were also observed. However, no new products compared to α-pinene alone with sulfated kaolinite was observed. Several peaks containing NSO were observed in both neg- and pos-ESI modes. However, similar to the case of hematite, here also no peak was assigned to a particular NOS compound due to the complexity of HRMS and MS/MS data. Overall, the current study suggests the formation of a unique mixture of ON and NOS and other oxidation products from the reactions of gas-phase NO_2 with adsorbed α-pinene-OS on mineral surfaces. Future research studies are recommended for understanding the reactions of NO_2 with VOC-derived OS adsorbed on mineral surfaces to better understand these reaction pathways. In particular, these studies can benefit from computational analyses. Quantification of identified surface products was not conducted in the current study due to the lack of availability of suitable standards.

CONCLUSIONS AND ATMOSPHERIC IMPLICATIONS

The reactions of α-pinene on sulfated hematite and kaolinite surfaces at 296 K yield several different OS and oxidation products of α-pinene. Kaolinite surfaces produce pinonalde-hyde and several OS compounds with a pinonaldehyde moiety, whereas all OS identified on hematite retained the α-pinene moiety, highlighting the underlying differences in the role of mineralogy and surface-specific chemistry. The adsorbed α-pinene-OS reacts with HNO_3 or NO_2 to produce more OS, multiple ON, and NOS products on surfaces. The proposed formation pathways of these OS occur via an adsorbed sulfite/sulfate species. The formation of ON and NOS compounds in the presence of HNO_3 suggests the addition of HNO_3, nucleophilic attacks by nitrates on OS, and reactions between ON and OS on the surface. Among other products, $C_{10}H_{17}NSO_7$, commonly known as NOS-295, was observed on both surfaces from reactions of OS with HNO_3. On hematite, OS ($C_9H_{14}SO_6$) and NOS ($C_{19}H_{32}NSO_{10}$) were observed, indicating the formation of C_9 compounds in the presence of HNO_3, thus underscoring the specific roles of mineral surfaces. The majority of surface products identified from the reactions of OS with NO_2 on both surfaces were either OS or oxidized α-pinene derivatives, along with evidence of the formation of NOS.

Overall, this study shows how mineral dust aerosol surface can interact with inorganic and organic gas-phase compounds to yield a wide range of compounds important for secondary organic aerosol surfaces. These data show that surfaces can interact with gas-phase SO_2 that then lead to OS surface products in the presence of ubiquitous organic compounds
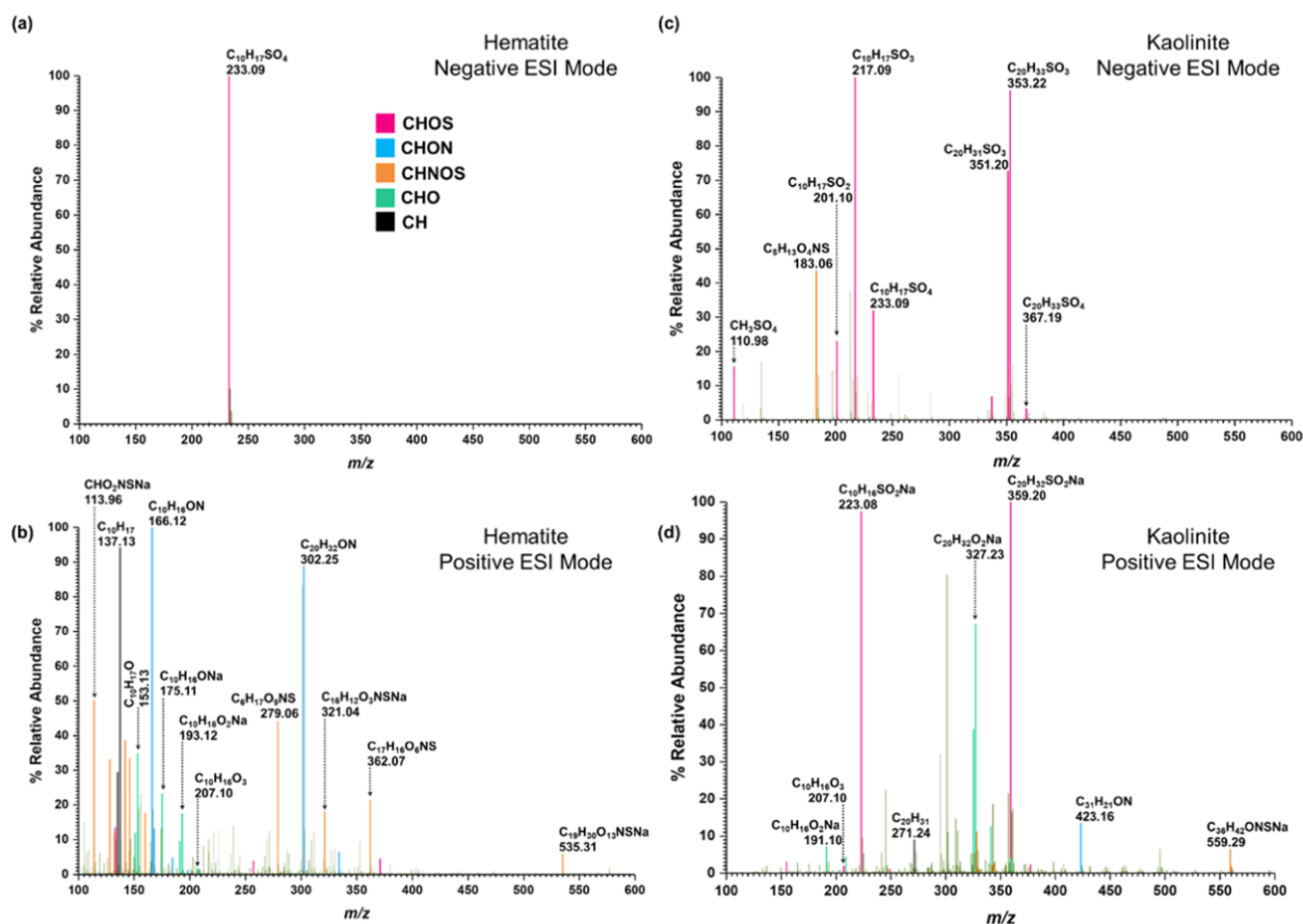
Figure 5. HRMS patterns in both positive $[M + H]^+$ and negative $[M - H]^-$ ESI modes of surface-bound products from the reactions of adsorbed α-pinene-OS with NO_2(gas) on (a, b) hematite and (c, d) kaolinite. Confirmed peaks are color-coded according to heteroatoms. Pink box solid—CHOS; blue box solid—CHON; orange box solid—CHNOS; green box solid—CHO; black box solid—CH.

such as α-pinene and then further can yield ON and NOS compounds when gas-phase nitrogen oxides are present. Most notable is that the specific products that form are mineral specific. Additionally, some of the SOAs observed in this study have been repeatedly observed in field studies; yet, formation pathways are poorly understood. In the environment, VOCs such as α-pinene are ubiquitous. During dust transport and urban dust episodes, these VOCs and trace gas pollutants such as NO_2 and SO_2 can interact with each other, forming more highly functional, less volatile compounds as shown here on two different mineral surfaces under dry conditions. As water plays an important role in heterogeneous chemistry,[53] it is important to further investigate how adsorbed water molecules impact these reactions. This study suggests heterogeneous reactions are possible pathways for the formation of these OS, ON, and NOS compounds but we also note the importance of extending this to different environmental conditions (e.g., relative humidity and solar radiation) on these formation pathways.

ASSOCIATED CONTENT

Supporting Information

The Supporting Information is available free of charge at https://pubs.acs.org/doi/10.1021/acsearthspacechem.2c00259.

FTIR spectra of sulfated mineral surfaces (Figure S1); vibrational frequencies of different adsorbed sulfur-containing species on hematite and kaolinite (Table S1); and MS/MS analysis of parent peaks for the identified compounds (Table S2) (PDF)

AUTHOR INFORMATION

Corresponding Author

Vicki H. Grassian − *Department of Chemistry and Biochemistry, University of California San Diego, La Jolla, California 92093, United States;* orcid.org/0000-0001-5052-0045; Email: vhgrassian@ucsd.edu

Author

Eshani Hettiarachchi − *Department of Chemistry and Biochemistry, University of California San Diego, La Jolla, California 92093, United States;* orcid.org/0000-0003-4293-770X

Complete contact information is available at:
https://pubs.acs.org/10.1021/acsearthspacechem.2c00259

Notes

The authors declare no competing financial interest.

■ REFERENCES

(1) Pye, H. O. T.; Ward-Caviness, C. K.; Murphy, B. N.; Appel, K. W.; Seltzer, K. M. Secondary Organic Aerosol Association with Cardiorespiratory Disease Mortality in the United States. *Nat. Commun.* **2021**, *12*, No. 7215.

(2) Liu, J.; Chu, B.; Chen, T.; Zhong, C.; Liu, C.; Ma, Q.; Ma, J.; Zhang, P.; He, H. Secondary Organic Aerosol Formation Potential from Ambient Air in Beijing: Effects of Atmospheric Oxidation Capacity at Different Pollution Levels. *Environ. Sci. Technol.* **2021**, *55*, 4565−4572.

(3) Wong, C.; Vite, D.; Nizkorodov, S. A. Stability of α-Pinene and d-Limonene Ozonolysis Secondary Organic Aerosol Compounds Toward Hydrolysis and Hydration. *ACS Earth Space Chem.* **2021**, *5*, 2555−2564.

(4) Khan, F.; Kwapiszewska, K.; Zhang, Y.; Chen, Y.; Lambe, A. T.; Kołodziejczyk, A.; Jalal, N.; Rudzinski, K.; Martínez-Romero, A.; Fry, R. C.; et al. Toxicological Responses of α-Pinene-Derived Secondary Organic Aerosol and Its Molecular Tracers in Human Lung Cell Lines. *Chem. Res. Toxicol.* **2021**, *34*, 817−832.

(5) Ge, S.; Wang, G.; Zhang, S.; Li, D.; Xie, Y.; Wu, C.; Yuan, Q.; Chen, J.; Zhang, H. Abundant NH_3 in China Enhances Atmospheric HONO Production by Promoting the Heterogeneous Reaction of SO_2 with NO_2. *Environ. Sci. Technol.* **2019**, *53*, 14339−14347.

(6) Lopez-Hilfiker, F. D.; Mohr, C.; D'Ambro, E. L.; Lutz, A.; Riedel, T. P.; Gaston, C. J.; Iyer, S.; Zhang, Z.; Gold, A.; Surratt, J. D.; et al. Molecular Composition and Volatility of Organic Aerosol in the Southeastern U.S.: Implications for IEPOX Derived SOA. *Environ. Sci. Technol.* **2016**, *50*, 2200−2209.

(7) Hu, W.; Zhou, H.; Chen, W.; Ye, Y.; Pan, T.; Wang, Y.; Song, W.; Zhang, H.; Deng, W.; Zhu, M.; et al. Oxidation Flow Reactor Results in a Chinese Megacity Emphasize the Important Contribution of S/IVOCs to Ambient SOA Formation. *Environ. Sci. Technol.* **2021**, *56*, 6880−6893.

(8) Salvador, C. M.; Chou, C. C.-K.; Cheung, H.-C.; Ho, T.-T.; Tsai, C.-Y.; Tsao, T.-M.; Tsai, M.-J.; Su, T.-C. Measurements of Submicron Organonitrate Particles: Implications for the Impacts of NOx Pollution in a Subtropical Forest. *Atmos. Res.* **2020**, *245*, No. 105080.

(9) Zhu, Q.; Cao, L. M.; Tang, M. X.; Huang, X. F.; Saikawa, E.; He, L. Y. Characterization of Organic Aerosol at a Rural Site in the North China Plain Region: Sources, Volatility and Organonitrates. *Adv. Atmos. Sci.* **2021**, *38*, 1115−1127.

(10) Brüggemann, M.; Xu, R.; Tilgner, A.; Kwong, K. C.; Mutzel, A.; Poon, H. Y.; Otto, T.; Schaefer, T.; Poulain, L.; Chan, M. N.; et al. Organosulfates in Ambient Aerosol: State of Knowledge and Future Research Directions on Formation, Abundance, Fate, and Importance. *Environ. Sci. Technol.* **2020**, *54*, 3767−3782.

(11) Xie, Q.; Su, S.; Chen, J.; Dai, Y.; Yue, S.; Su, H.; Tong, H.; Zhao, W.; Ren, L.; Xu, Y.; et al. Increase of Nitrooxy Organosulfates in Firework-Related Urban Aerosols during Chinese New Year's Eve. *Atmos. Chem. Phys.* **2021**, *21*, 11453−11465.

(12) Glasius, M.; Goldstein, A. H. Recent Discoveries and Future Challenges in Atmospheric Organic Chemistry. *Environ. Sci. Technol.* **2016**, *50*, 2754−2764.

(13) Guenther, A.; Karl, T.; Harley, P.; Wiedinmyer, C.; Palmer, P. I.; Geron, C. Estimates of Global Terrestrial Isoprene Emissions Using MEGAN (Model of Emissions of Gases and Aerosols from Nature). *Atmos. Chem. Phys.* **2006**, *6*, 3181−3210.

(14) Geron, C.; Rasmussen, R.; Arnts, R. R.; Guenther, A. A Review and Synthesis of Monoterpene Speciation from Forests in the United States. *Atmos. Environ.* **2000**, *34*, 1761−1781.

(15) Ehn, M.; Thornton, J. A.; Kleist, E.; Sipilä, M.; Junninen, H.; Pullinen, I.; Springer, M.; Rubach, F.; Tillmann, R.; Lee, B.; et al. A Large Source of Low-Volatility Secondary Organic Aerosol. *Nature* **2014**, *506*, 476−479.

(16) Surratt, J. D.; Kroll, J. H.; Kleindienst, T. E.; Edney, E. O.; Claeys, M.; Sorooshian, A.; Ng, N. L.; Offenberg, J. H.; Lewandowski, M.; Jaoui, M.; et al. Evidence for Organosulfates in Secondary Organic Aerosol. *Environ. Sci. Technol.* **2007**, *41*, 517−527.

(17) Iinuma, Y.; Müller, C.; Berndt, T.; Böge, O.; Claeys, M.; Herrmann, H. Evidence for the Existence of Organosulfates from β-Pinene Ozonolysis in Ambient Secondary Organic Aerosol. *Environ. Sci. Technol.* **2007**, *41*, 6678−6683.

(18) Stone, E. A.; Yang, L.; Yu, L. E.; Rupakheti, M. Characterization of Organosulfates in Atmospheric Aerosols at Four Asian Locations. *Atmos. Environ.* **2012**, *47*, 323−329.

(19) He, Q. F.; Ding, X.; Wang, X. M.; Yu, J. Z.; Fu, X. X.; Liu, T. Y.; Zhang, Z.; Xue, J.; Chen, D. H.; Zhong, L. J.; Donahue, N. M. Organosulfates from Pinene and Isoprene over the Pearl River Delta, South China: Seasonal Variation and Implication in Formation Mechanisms. *Environ. Sci. Technol.* **2014**, *48*, 9236−9245.

(20) Chan, M. N.; Surratt, J. D.; Chan, A. W. H.; Schilling, K.; Offenberg, J. H.; Lewandowski, M.; Edney, E. O.; Kleindienst, T. E.; Jaoui, M.; Edgerton, E. S.; et al. Influence of Aerosol Acidity on the Chemical Composition of Secondary Organic Aerosol from β-Caryophyllene. *Atmos. Chem. Phys.* **2011**, *11*, 1735−1751.

(21) Gao, S.; Ng, N. L.; Keywood, M.; Varutbangkul, V.; Bahreini, R.; Nenes, A.; He, J.; Yoo, K. Y.; Beauchamp, J. L.; Hodyss, R. P.; et al. Particle Phase Acidity and Oligomer Formation in Secondary Organic Aerosol. *Environ. Sci. Technol.* **2004**, *38*, 6582−6589.

(22) Surratt, J. D.; Gómez-González, Y.; Chan, A. W. H.; Vermeylen, R.; Shahgholi, M.; Kleindienst, T. E.; Edney, E. O.; Offenberg, J. H.; Lewandowski, M.; Jaoui, M.; et al. Organosulfate Formation in Biogenic Secondary Organic Aerosol. *J. Phys. Chem. A* **2008**, *112*, 8345−8378.

(23) Perri, M. J.; Lim, Y. B.; Seitzinger, S. P.; Turpin, B. J. Organosulfates from Glycolaldehyde in Aqueous Aerosols and Clouds: Laboratory Studies. *Atmos. Environ.* **2010**, *44*, 2658−2664.

(24) Fleming, L. T.; Ali, N. N.; Blair, S. L.; Roveretto, M.; George, C.; Nizkorodov, S. A. Formation of Light-Absorbing Organosulfates during Evaporation of Secondary Organic Material Extracts in the Presence of Sulfuric Acid. *ACS Earth Space Chem.* **2019**, *3*, 947−957.

(25) Schmidt, M.; van Beek, S. M. J.; Abou-Ghanem, M.; Oliynyk, A. O.; Locock, A. J.; Styler, S. A. Production of Atmospheric Organosulfates via Mineral-Mediated Photochemistry. *ACS Earth Space Chem.* **2019**, *3*, 424−431.

(26) Duporté, G.; Flaud, P. M.; Kammer, J.; Geneste, E.; Augagneur, S.; Pangui, E.; Lamkaddam, H.; Gratien, A.; Doussin, J. F.; Budzinski, H.; et al. Experimental Study of the Formation of Organosulfates from α-Pinene Oxidation. 2. Time Evolution and Effect of Particle Acidity. *J. Phys. Chem. A* **2020**, *124*, 409−421.

(27) Duporté, G.; Flaud, P. M.; Geneste, E.; Augagneur, S.; Pangui, E.; Lamkaddam, H.; Gratien, A.; Doussin, J. F.; Budzinski, H.; Villenave, E.; et al. Experimental Study of the Formation of Organosulfates from α-Pinene Oxidation. Part I: Product Identification, Formation Mechanisms and Effect of Relative Humidity. *J. Phys. Chem. A* **2016**, *120*, 7909−7923.

(28) Wang, Y.; Ma, Y.; Li, X.; Kuang, B. Y.; Huang, C.; Tong, R.; Yu, J. Z. Monoterpene and Sesquiterpene α-Hydroxy Organosulfates: Synthesis, MS/MS Characteristics, and Ambient Presence. *Environ. Sci. Technol.* **2019**, *53*, 12278−12290.

(29) Tolocka, M. P.; Turpin, B. Contribution of Organosulfur Compounds to Organic Aerosol Mass. *Environ. Sci. Technol.* **2012**, *46*, 7978−7983.

(30) Farmer, D. K.; Matsunaga, A.; Docherty, K. S.; Surratt, J. D.; Seinfeld, J. H.; Ziemann, P. J.; Jimenez, J. L. Response of an Aerosol Mass Spectrometer to Organonitrates and Organosulfates and Implications for Atmospheric Chemistry. *Proc. Natl. Acad. Sci. U.S.A.* **2010**, *107*, 6670−6675.

(31) Rollins, A. W.; Kiendler-Scharr, A.; Fry, J. L.; Brauers, T.; Brown, S. S.; Dorn, H.-P.; Dubé, W. P.; Fuchs, H.; Mensah, A.; Mentel, T. F.; et al. Isoprene Oxidation by Nitrate Radical: Alkyl

Nitrate and Secondary Organic Aerosol Yields. *Atmos. Chem. Phys.* **2009**, *9*, 6685–6703.

(32) Ma, S. X.; Rindelaub, J. D.; McAvey, K. M.; Gagare, P. D.; Nault, B. A.; Ramachandran, P. V.; Shepson, P. B. α-Pinene Nitrates: Synthesis, Yields and Atmospheric Chemistry. *Atmos. Chem. Phys.* **2011**, *11*, 6337–6347.

(33) Perraud, V.; Bruns, E. A.; Ezell, M. J.; Johnson, S. N.; Greaves, J.; Finlayson-Pitts, B. J. Identification of Organic Nitrates in the NO₃ Radical Initiated Oxidation of α-Pinene by Atmospheric Pressure Chemical Ionization Mass Spectrometry. *Environ. Sci. Technol.* **2010**, *44*, 5887–5893.

(34) Takeuchi, M.; Ng, N. L. Organic Nitrates and Secondary Organic Aerosol (SOA) Formation from Oxidation of Biogenic Volatile Organic Compounds. In *ACS Symposium Series*, 2018; Vol 1299, pp 105–125.

(35) Rindelaub, J. D.; McAvey, K. M.; Shepson, P. B. The Photochemical Production of Organic Nitrates from α-Pinene and Loss via Acid-Dependent Particle Phase Hydrolysis. *Atmos. Environ.* **2015**, *100*, 193–201.

(36) Saleh, R.; Donahue, N. M.; Robinson, A. L. Time Scales for Gas-Particle Partitioning Equilibration of Secondary Organic Aerosol Formed from Alpha-Pinene Ozonolysis. *Environ. Sci. Technol.* **2013**, *47*, 5588–5594.

(37) Masoud, C. G.; Ruiz, L. H. Chlorine-Initiated Oxidation of α-Pinene: Formation of Secondary Organic Aerosol and Highly Oxygenated Organic Molecules. *ACS Earth Space Chem.* **2021**, *5*, 2307–2319.

(38) Takeuchi, M.; Ng, N. L. Chemical Composition and Hydrolysis of Organic Nitrate Aerosol Formed from Hydroxyl and Nitrate Radical Oxidation of Alpha-Pinene and Beta-Pinene. *Atmos. Chem. Phys.* **2019**, *19*, 12749–12766.

(39) Friedman, B.; Farmer, D. K. SOA and Gas Phase Organic Acid Yields from the Sequential Photooxidation of Seven Monoterpenes. *Atmos. Environ.* **2018**, *187*, 335–345.

(40) Hettiarachchi, E.; Grassian, V. H. Heterogeneous Reactions of α-Pinene on Mineral Surfaces: Formation of Organonitrates and α-Pinene Oxidation Products. *J. Phys. Chem. A* **2022**, *126*, 4068–4079.

(41) Liggio, J.; Li, S. M. Reactive Uptake of Pinonaldehyde on Acidic Aerosols. *J. Geophys. Res.* **2006**, *111*, No. D24303.

(42) Kristensen, K.; Glasius, M. Organosulfates and Oxidation Products from Biogenic Hydrocarbons in Fine Aerosols from a Forest in North West Europe during Spring. *Atmos. Environ.* **2011**, *45*, 4546–4556.

(43) Kandler, K.; Benker, N.; Bundke, U.; Cuevas, E.; Ebert, M.; Knippertz, P.; Rodríguez, S.; Schütz, L.; Weinbruch, S. Chemical Composition and Complex Refractive Index of Saharan Mineral Dust at Izaña, Tenerife (Spain) Derived by Electron Microscopy. *Atmos. Environ.* **2007**, *41*, 8058–8074.

(44) Martins-Costa, M. T. C.; Anglada, J. M.; Francisco, J. S.; Ruiz-López, M. F. Photochemistry of SO₂ at the Air−Water Interface: A Source of OH and HOSO Radicals. *J. Am. Chem. Soc.* **2018**, *140*, 12341–12344.

(45) Bozkurt, Z.; Üzmez, Ö. Ö.; Döğeroğlu, T.; Artun, G.; Gaga, E. O. Atmospheric Concentrations of SO₂, NO₂, Ozone and VOCs in Düzce, Turkey Using Passive Air Samplers: Sources, Spatial and Seasonal Variations and Health Risk Estimation. *Atmos. Pollut. Res.* **2018**, *9*, 1146–1156.

(46) Pinault, L.; Crouse, D.; Jerrett, M.; Brauer, M.; Tjepkema, M. Spatial Associations between Socioeconomic Groups and NO₂ Air Pollution Exposure within Three Large Canadian Cities. *Environ. Res.* **2016**, *147*, 373–382.

(47) Bozkurt, Z.; Doğan, G.; Arslanbaş, D.; Pekey, B.; Pekey, H.; Dumanoğlu, Y.; Bayram, A.; Tuncel, G. Determination of the Personal, Indoor and Outdoor Exposure Levels of Inorganic Gaseous Pollutants in Different Microenvironments in an Industrial City. *Environ. Monit. Assess.* **2015**, *187*, No. 590.

(48) Zhao, H.; Sheng, X.; Fabris, S.; Salahub, D. R.; Sun, T.; Du, L. Heterogeneous Reactions of SO₂ on the Hematite(0001) Surface. *J. Chem. Phys.* **2018**, *149*, No. 194703.

(49) Toledano, D. S.; Henrich, V. E. Kinetics of SO₂ adsorption on Photoexcited α-Fe₂O₃. *J. Phys. Chem. B* **2001**, *105*, 3872–3877.

(50) Baltrusaitis, J.; Cwiertny, D. M.; Grassian, V. H. Adsorption of Sulfur Dioxide on Hematite and Goethite Particle Surfaces. *Phys. Chem. Chem. Phys.* **2007**, *9*, No. 5542.

(51) Sonibare, J. A.; Akeredolu, F. A. A Theoretical Prediction of Non-Methane Gaseous Emissions from Natural Gas Combustion. *Energy Policy* **2004**, *32*, 1653–1665.

(52) Tang, M.; Cziczo, D. J.; Grassian, V. H. Interactions of Water with Mineral Dust Aerosol: Water Adsorption, Hygroscopicity, Cloud Condensation, and Ice Nucleation. *Chem. Rev.* **2016**, *116*, 4205–4259.

(53) Rubasinghege, G.; Grassian, V. H. Role(s) of Adsorbed Water in the Surface Chemistry of Environmental Interfaces. *Chem. Commun.* **2013**, *49*, No. 3071.

(54) Nanayakkara, C. E.; Larish, W. A.; Grassian, V. H. Titanium Dioxide Nanoparticle Surface Reactivity with Atmospheric Gases, CO₂, SO₂, and NO₂: Roles of Surface Hydroxyl Groups and Adsorbed Water in the Formation and Stability of Adsorbed Products. *J. Phys. Chem. C* **2014**, *118*, 23011–23021.

(55) Tang, M.; Larish, W. A.; Fang, Y.; Gankanda, A.; Grassian, V. H. Heterogeneous Reactions of Acetic Acid with Oxide Surfaces: Effects of Mineralogy and Relative Humidity. *J. Phys. Chem. A* **2016**, *120*, 5609–5616.

(56) Fang, Y.; Tang, M.; Grassian, V. H. Competition between Displacement and Dissociation of a Strong Acid Compared to a Weak Acid Adsorbed on Silica Particle Surfaces: The Role of Adsorbed Water. *J. Phys. Chem. A* **2016**, *120*, 4016–4024.

(57) Fang, Y.; Lesnicki, D.; Wall, K. J.; Gaigeot, M. P.; Sulpizi, M.; Vaida, V.; Grassian, V. H. Heterogeneous Interactions between Gas-Phase Pyruvic Acid and Hydroxylated Silica Surfaces: A Combined Experimental and Theoretical Study. *J. Phys. Chem. A* **2019**, *123*, 983–991.

(58) Goodman, A. L.; Bernard, E. T.; Grassian, V. H. Spectroscopic Study of Nitric Acid and Water Adsorption on Oxide Particles: Enhanced Nitric Acid Uptake Kinetics in the Presence of Adsorbed Water. *J. Phys. Chem. A* **2001**, *105*, 6443–6457.

(59) Goodman, A. L.; Underwood, G. M.; Grassian, V. H. A Laboratory Study of the Heterogeneous Reaction of Nitric Acid on Calcium Carbonate Particles. *J. Geophys. Res.: Atmos.* **2000**, *105*, 29053–29064.

(60) Goodman, A. L.; Li, P.; Usher, C. R.; Grassian, V. H. Heterogeneous Uptake of Sulfur Dioxide On Aluminum and Magnesium Oxide Particles. *J. Phys. Chem. A* **2001**, *105*, 6109–6120.

(61) Nanayakkara, C. E.; Pettibone, J.; Grassian, V. H. Sulfur Dioxide Adsorption and Photooxidation on Isotopically-Labeled Titanium Dioxide Nanoparticle Surfaces: Roles of Surface Hydroxyl Groups and Adsorbed Water in the Formation and Stability of Adsorbed Sulfite and Sulfate. *Phys. Chem. Chem. Phys.* **2012**, *14*, 6957–6966.

(62) Wang, T.; Liu, Y.; Deng, Y.; Fu, H.; Zhang, L.; Chen, J. Adsorption of SO₂ on Mineral Dust Particles Influenced by Atmospheric Moisture. *Atmos. Environ.* **2018**, *191*, 153–161.

(63) Socrates, G. *Infrared and Raman Characteristic Group Frequencies*, 3rd ed.; Wiley, 2000.

(64) Bondy, A. L.; Craig, R. L.; Zhang, Z.; Gold, A.; Surratt, J. D.; Ault, A. P. Isoprene-Derived Organosulfates: Vibrational Mode Analysis by Raman Spectroscopy, Acidity-Dependent Spectral Modes, and Observation in Individual Atmospheric Particles. *J. Phys. Chem. A* **2018**, *122*, 303–315.

(65) Hyttinen, N.; Elm, J.; Malila, J.; Calderón, S. M.; Prisle, N. L. Thermodynamic Properties of Isoprene- and Monoterpene-Derived Organosulfates Estimated with COSMOtherm. *Atmos. Chem. Phys.* **2020**, *20*, 5679–5696.

(66) Liggio, J.; Li, S.-M. Organosulfate Formation during the Uptake of Pinonaldehyde on Acidic Sulfate Aerosols. *Geophys. Res. Lett.* **2006**, *33*, No. L13808.

(67) Xu, R.; Ng, S. I. M.; Chow, W. S.; Wong, Y. K.; Wang, Y.; Lai, D.; Yao, Z.; So, P.-K.; Yu, J. Z.; Chan, M. N. Chemical

Transformation of α-Pinene-Derived Organosulfate via Heterogeneous OH Oxidation: Implications for Sources and Environmental Fates of Atmospheric Organosulfates. *Atmos. Chem. Phys.* **2022**, *22*, 5685–5700.

(68) Rindelaub, J. D.; Wiley, J. S.; Cooper, B. R.; Shepson, P. B. Chemical Characterization of α-Pinene Secondary Organic Aerosol Constituents Using Gas Chromatography, Liquid Chromatography, and Paper Spray-Based Mass Spectrometry Techniques. *Rapid Commun. Mass Spectrom.* **2016**, *30*, 1627–1638.

(69) Ye, Y.; Zhan, H.; Yu, X.; Li, J.; Wang, X.; Xie, Z. Detection of Organosulfates and Nitrooxy-Organosulfates in Arctic and Antarctic Atmospheric Aerosols, Using Ultra-High Resolution FT-ICR Mass Spectrometry. *Sci. Total Environ.* **2021**, *767*, No. 144339.

(70) Lee, A.; Goldstein, A. H.; Kroll, J. H.; Ng, N. L.; Varutbangkul, V.; Flagan, R. C.; Seinfeld, J. H. Gas-Phase Products and Secondary Aerosol Yields from the Photooxidation of 16 Different Terpenes. *J. Geophys. Res.* **2006**, *111*, No. D17305.

(71) Eddingsaas, N. C.; Loza, C. L.; Yee, L. D.; Seinfeld, J. H.; Wennberg, P. O. α-Pinene Photooxidation under Controlled Chemical Conditions − Part 1: Gas-Phase Composition in Low- and High-NOx; Environments. *Atmos. Chem. Phys.* **2012**, *12*, 6489–6504.

(72) Li, H.; Riva, M.; Rantala, P.; Heikkinen, L.; Daellenbach, K.; Krechmer, J. E.; Flaud, P.-M.; Worsnop, D.; Kulmala, M.; Villenave, E.; et al. Terpenes and Their Oxidation Products in the French Landes Forest: Insights from Vocus PTR-TOF Measurements. *Atmos. Chem. Phys.* **2020**, *20*, 1941–1959.

(73) Kanakidou, M.; Seinfeld, J. H.; Pandis, S. N.; Barnes, I.; Dentener, F. J.; Facchini, M. C.; Van Dingenen, R.; Ervens, B.; Nenes, A.; Nielsen, C. J.; et al. Organic Aerosol and Global Climate Modelling: A Review. *Atmos. Chem. Phys.* **2005**, *5*, 1053–1123.

(74) Wozniak, A. S.; Bauer, J. E.; Sleighter, R. L.; Dickhut, R. M.; Hatcher, P. G. Technical Note: Molecular Characterization of Aerosol-Derived Water Soluble Organic Carbon Using Ultrahigh Resolution Electrospray Ionization Fourier Transform Ion Cyclotron Resonance Mass Spectrometry. *Atmos. Chem. Phys.* **2008**, *8*, 5099–5111.

(75) Caudillo, L.; Rörup, B.; Heinritzi, M.; Marie, G.; Simon, M.; Wagner, A. C.; Müller, T.; Granzin, M.; Amorim, A.; Ataei, F.; et al. Chemical Composition of Nanoparticles from Alpha-Pinene Nucleation and the Influence of Isoprene and Relative Humidity at Low Temperature. *Atmos. Chem. Phys.* **2021**, *21*, 17099–17114.

(76) Baboomian, V. J.; Gu, Y.; Nizkorodov, S. A. Photodegradation of Secondary Organic Aerosols by Long-Term Exposure to Solar Actinic Radiation. *ACS Earth Space Chem.* **2020**, *4*, 1078–1089.

(77) Zhao, Y.; Thornton, J. A.; Pye, H. O. T. Quantitative Constraints on Autoxidation and Dimer Formation from Direct Probing of Monoterpene-Derived Peroxy Radical Chemistry. *Proc. Natl. Acad. Sci. U.S.A.* **2018**, *115*, 12142–12147.

(78) Passananti, M.; Kong, L.; Shang, J.; Dupart, Y.; Perrier, S.; Chen, J.; Donaldson, D. J.; George, C. Organosulfate Formation through the Heterogeneous Reaction of Sulfur Dioxide with Unsaturated Fatty Acids and Long-Chain Alkenes. *Angew. Chem., Int. Ed.* **2016**, *55*, 10336–10339.

(79) Shang, J.; Passananti, M.; Dupart, Y.; Ciuraru, R.; Tinel, L.; Rossignol, S.; Perrier, S.; Zhu, T.; George, C. SO₂ Uptake on Oleic Acid: A New Formation Pathway of Organosulfur Compounds in the Atmosphere. *Environ. Sci. Technol. Lett.* **2016**, *3*, 67–72.

(80) Lederer, M. R.; Staniec, A. R.; Fuentes, Z. L. C.; Van Ry, D. A.; Hinrichs, R. Z. Heterogeneous Reactions of Limonene on Mineral Dust: Impacts of Adsorbed Water and Nitric Acid. *J. Phys. Chem. A* **2016**, *120*, 9545–9556.

(81) Xu, L.; Yang, Z.; Tsona, N. T.; Wang, X.; George, C.; Du, L. Anthropogenic−Biogenic Interactions at Night: Enhanced Formation of Secondary Aerosols and Particulate Nitrogen- and Sulfur-Containing Organics from β-Pinene Oxidation. *Environ. Sci. Technol.* **2021**, *55*, 7794–7807.

(82) Czoschke, N.; Jang, M. Markers of Heterogeneous Reaction Products in α-Pinene Ozone Secondary Organic Aerosol. *Atmos. Environ.* **2006**, *40*, 5629–5639.

(83) Lee, S.; Jang, M.; Kamens, R. M. SOA Formation from the Photooxidation of α-Pinene in the Presence of Freshly Emitted Diesel Soot Exhaust. *Atmos. Environ.* **2004**, *38*, 2597–2605.

(84) Ma, Y.; Brooks, S. D.; Vidaurre, G.; Khalizov, A. F.; Wang, L.; Zhang, R. Rapid Modification of Cloud-Nucleating Ability of Aerosols by Biogenic Emissions. *Geophys. Res. Lett.* **2013**, *40*, 6293–6297.

(85) Zhang, X.; McVay, R. C.; Huang, D. D.; Dalleska, N. F.; Aumont, B.; Flagan, R. C.; Seinfeld, J. H. Formation and Evolution of Molecular Products in α-Pinene Secondary Organic Aerosol. *Proc. Natl. Acad. Sci. U.S.A.* **2015**, *112*, 14168–14173.

(86) Qi, L.; Chen, M.; Stefenelli, G.; Pospisilova, V.; Tong, Y.; Bertrand, A.; Hueglin, C.; Ge, X.; Baltensperger, U.; Prévôt, A. S. H.; Slowik, J. G. Organic Aerosol Source Apportionment in Zurich Using an Extractive Electrospray Ionization Time-of-Flight Mass Spectrometer (EESI-TOF-MS) − Part 2: Biomass Burning Influences in Winter. *Atmos. Chem. Phys.* **2019**, *19*, 8037–8062.

(87) Wang, Y.; Tong, R.; Yu, J. Z. Chemical Synthesis of Multifunctional Air Pollutants: Terpene-Derived Nitrooxy Organosulfates. *Environ. Sci. Technol.* **2021**, *55*, 8573–8582.

(88) Bryant, D. J.; Elzein, A.; Newland, M.; White, E.; Swift, S.; Watkins, A.; Deng, W.; Song, W.; Wang, S.; Zhang, Y.; et al. Importance of Oxidants and Temperature in the Formation of Biogenic Organosulfates and Nitrooxy Organosulfates. *ACS Earth Space Chem.* **2021**, *5*, 2291–2306.

(89) Le Breton, M.; Wang, Y.; Hallquist, Å. M.; Pathak, R. K.; Zheng, J.; Yang, Y.; Shang, D.; Glasius, M.; Bannan, T. J.; Liu, Q.; et al. Online Gas- and Particle-Phase Measurements of Organosulfates, Organosulfonates and Nitrooxy Organosulfates in Beijing Utilizing a FIGAERO ToF-CIMS. *Atmos. Chem. Phys.* **2018**, *18*, 10355–10371.

(90) Surh, Y. J.; Liem, A.; Miller, J. A.; Tannenbaum, S. R. 5-Sulfooxymethylfurfural as a Possible Ultimate Mutagenic and Carcinogenic Metabolite of the Maillard Reaction Product, 5-Hydroxymethylfurfural. *Carcinogenesis* **1994**, *15*, 2375–2377.

(91) Harvey, B. G.; Wright, M. E.; Quintana, R. L. High-Density Renewable Fuels Based on the Selective Dimerization of Pinenes. *Energy Fuels* **2010**, *24*, 267–273.

(92) Zhang, S.; Xu, C.; Zhai, G.; Zhao, M.; Xian, M.; Jia, Y.; Yu, Z.; Liu, F.; Jian, F.; Sun, W. Bifunctional Catalyst Pd−Al-MCM-41 for Efficient Dimerization−Hydrogenation of β-Pinene in One Pot. *RSC Adv.* **2017**, *7*, 47539–47546.

(93) Molteni, U.; Simon, M.; Heinritzi, M.; Hoyle, C. R.; Bernhammer, A. K.; Bianchi, F.; Breitenlechner, M.; Brilke, S.; Dias, A.; Duplissy, J.; et al. Formation of Highly Oxygenated Organic Molecules from α-Pinene Ozonolysis: Chemical Characteristics, Mechanism, and Kinetic Model Development. *ACS Earth Space Chem.* **2019**, *3*, 873–883.